ORIGINAL RESEARCH

Catalytically active bovine serum amine oxidase bound to fluorescent and magnetically drivable nanoparticles

Giulietta Sinigaglia[1]
Massimiliano Magro[1]
Giovanni Miotto[1]
Sara Cardillo[1]
Enzo Agostinelli[2,3]
Radek Zboril[4]
Eris Bidollari[2,3]
Fabio Vianello[1]

[1]Department of Biological Chemistry, University of Padua, Padua, Italy; [2]Istituto Pasteur-Fondazione Cenci Bolognetti, Department of Biochemical Sciences "A. Rossi Fanelli", SAPIENZA University of Rome, Rome, Italy; [3]CNR, Institute Biology and Molecular Pathology, Rome, Italy; [4]Regional Centre of Advanced Technologies and Materials, Department of Physical Chemistry, Palacky University, Olomouc, Czech Republic

Correspondence: Fabio Vianello
Department of Comparative Biomedicine and Food Science, University of Padua
Agripolis – Viale dell'Università 16, Legnaro, 35020 (PD), Italy
Tel +39 049 827 6863
Fax +39 049 807 3310
Email fabio.vianello@unipd.it

Abstract: Novel superparamagnetic surface-active maghemite nanoparticles (SAMNs) characterized by a diameter of 10 ± 2 nm were modified with bovine serum amine oxidase, which used rhodamine B isothiocyanate (RITC) adduct as a fluorescent spacer-arm. A fluorescent and magnetically drivable adduct comprised of bovine serum copper-containing amine oxidase (SAMN–RITC–BSAO) that immobilized on the surface of specifically functionalized magnetic nanoparticles was developed. The multifunctional nanomaterial was characterized using transmission electron microscopy, infrared spectroscopy, mass spectrometry, and activity measurements. The results of this study demonstrated that bare magnetic nanoparticles form stable colloidal suspensions in aqueous solutions. The maximum binding capacity of bovine serum amine oxidase was approximately 6.4 mg g^{-1} nanoparticles. The immobilization procedure reduced the catalytic activity of the native enzyme to $30\% \pm 10\%$ and the Michaelis constant was increased by a factor of 2. We suggest that the SAMN–RITC–BSAO complex, characterized by a specific activity of 0.81 IU g^{-1}, could be used in the presence of polyamines to create a fluorescent magnetically drivable H$_2$O$_2$ and aldehydes-producing system. Selective tumor cell destruction is suggested as a potential future application of this system.

Keywords: amine oxidase, hydrogen peroxide production, superparamagnetic nanoparticles, rhodamine isothiocyanate, fluorescent nanoparticles, fluorescent nanocatalyst

As a result of the rapid development of nanotechnology, magnetic nanoparticles are now widely studied. It has long been known that the physicochemical properties of magnetic nanoparticles can be vastly different from the properties of the corresponding bulk material.[1]

In comparison to micro- or submicrometric size particles, the advantage of using nanometric size particles is that they have a larger surface area that can be used to attach biomolecules. These biomolecules will enable the preparation of nanostructured biomaterial with a high loading per mass unit and the possibility of immobilizing biomolecules.

Magnetic separation is an interesting tool that is used in bioassays because, when compared to conventional chromatographic methods, the magnetic beads enable the isolation or extraction of a target molecule with higher efficiencies through the application of an external magnetic field.[2–4] Due to the good biocompatibility and adequate functional groups for chemical fixation, magnetic nanoparticles modified on the surface by various recognition polymers can be used to immobilize specific biomolecules. Additionally, they are employed as a solid adsorbent and as magnetic separation of support from the reaction mixture.[5] Magnetic nanoparticles are applicable

in many areas such as the immobilization of proteins and enzymes,[6] bioseparation,[7] immunoassay,[8] drug delivery,[9] and biosensors.[10]

We have developed a new method to synthesize superparamagnetic nanoparticles constituted of stoichiometric maghemite (γ-Fe_2O_3) with a dimension of approximately 10 nm. These nanoparticles are characterized by specific chemical behavior without any superficial modification or coating derivatization. These bare iron nanoparticles are stable in water for several months as colloidal suspensions. They also present a high average magnetic moment and can be easily derivatized to immobilize specific organic molecules in a solution.[11,12]

The aim of this present work is to combine the advantages of immobilized proteins on nanomaterials and the easy operation of magnetic nanoparticles to develop an inexpensive and simple amine oxidase-based magnetic nanocatalyst tagged with a fluorescent probe.

Copper containing amine oxidases, Cu-AO (EC 1.4.3.6), represents a heterogeneous class of enzymes (amine:oxygen oxidoreductase [deaminating] [copper-containing]) that is widely found in mammals, plants, and microorganisms.[13] There has been an increase in research interest in this class of enzymes because they are involved in polyamine metabolism and in numerous physiopathological processes.[14] A number of Cu-AOs have been purified to homogeneity and characterized. These enzymes share some fundamental structural properties. They both are glycosylated homodimers measuring 70–95 kDa. Depending on their source, each monomer contains one tightly bound Cu(II) ion and one carbonyl-type group as cofactors. These cofactors are either 6-hydroxydopa quinone (2,4,5-trihydroxyphenylalaninequinone) or lysine tyrosylquinone.[15,16]

These enzymes operate by abstracting two electrons from aromatic and aliphatic primary amines and transferring them to molecular oxygen. The following equation demonstrates how this process produces the corresponding aldehyde, ammonia, and hydrogen peroxide:

$$R\text{-}CH_2\text{-}NH_3^+ + O_2 + H_2O \xrightarrow{\text{Amine oxidase}}$$
$$R\text{-}CHO + NH_4^+ + H_2O_2$$
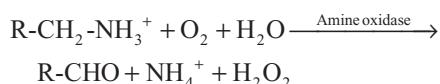
Despite their wide distribution, the physiological role of Cu-AOs is still unclear. Bovine serum amine oxidase (BSAO: EC 1.4.3.6) was used to generate cytotoxic polyamine metabolites. The oxidative deamination of spermine by BSAO generates H_2O_2, aldehydes, and ammonia.[17–19] Hydrogen peroxide and aldehydes induce

stress-activated signal transduction pathways, which leads to apoptotic and nonapoptotic cell death.[20,21] Exposure of tumor cells to purified BSAO and spermine causes a time-dependent decrease of cell viability[21] and impairs the growth of mouse melanoma.[22] Analogous to other radical forming processes, the formation of reactive oxygen species (ROS) and cytotoxic aldehydes from polyamines are currently being explored as a possible strategy in cancer therapy.[23] Moreover, hydrogen peroxide and aldehydes generated by BSAO/spermine enzymatic systems have been shown to overcome multidrug resistance (MDR) in human colon adenocarcinoma (LoVo)[24,25] and melanoma (M14) cells.[26] This is particularly interesting because one of the problems of conventional anticancer therapy is the development of drug resistance.

In the present work, we report a unique synthetic route of maghemite nanoparticles exhibiting excellent colloidal behavior without any additional organic or inorganic modification of their surface. These nanoparticles immobilized rhodamine B isothiocyanate (RITC), which acted as a fluorescent label, and a magnetically controllable rhodamine-based fluorescent nanocomposite has been synthesized as a result. Moreover, the rhodamine structure used in this research allows for the covalent attachment of various biomolecules. This has been demonstrated in the immobilization of BSAO. Acting as a monomolecular layer, the immobilized enzyme retains its catalytic activity towards oxidation of polyamines. The prepared fluorescent magnetically drivable nanocatalyst could be used as a nanodevice that selectively kills tumor cells by the in situ production of hydrogen peroxide and aldehydes.[27] In order to achieve this potential clinical application, our system offers the dual advantage of being easily removed by nanomaterial superparamagnetism and of being easily detectable by fluorescence.

Materials and methods
Chemicals
Chemicals were purchased at the highest commercially available purity and were used without further treatment. Iron(III) chloride hexahydrate (97%), sodium borohydride ($NaBH_4$), RITC, rhodamine 110, rhodamine B, fluorescein, fluorescein isothiocyanate (FITC), tetramethylammonium hydroxide, perchloric acid, and ammonia solution (35% in water) were obtained from Aldrich (Sigma-Aldrich, Milan, Italy). Spermine tetrahydrochloride was obtained from Fluka (Buchs, Switzerland).

Amine oxidase from bovine serum was purified to electrophoretic homogeneity according to Turini et al.[28] All of the

samples that were used had a minimum specific activity on benzylamine oxidation of 0.38 IU mg⁻¹. Assay was performed spectrophotometrically at 25°C by monitoring the formation of benzaldehyde at 250 nm absorbance ($\varepsilon = 1.25 \times 10^4\,M^{-1}cm^{-1}$). International Unit (IU) is defined as μmoles of substrate oxidized per minute.

Instrumentation

Optical spectroscopy and fluorescence measurements were respectively performed in 1 cm quartz cuvettes using a Cary 50 spectrophotometer and a Cary Eclipse fluorescence spectrometer (Varian Inc, Palo Alto, CA).

Fourier transform-infrared (FTIR) spectra were acquired using a Thermo Nicolet NEXUS 670 FTIR instrument (Thermo Fisher Scientific, Waltham, MA). Nanoparticle samples were homogenized with KBr powder and pelletized using an 8-ton hydraulic press. Microscopic characterizations of the native maghemite particles, as well as rhodamine-coated particles, were performed using transmission electron microscopy (TEM). TEM micrographs were obtained using a Tecnai 12 microscope (FEI, Portland, OR) operating at 120 kV with a point-to-point resolution of 1.9 Å.

Synthesis of iron oxide nanoparticles

A typical nanoparticle synthesis has already been described[11,12] and can be summarized as follows: $FeCl_3 \times 6H_2O$ (10.0 g, 37 mmol) was dissolved in MilliQ grade water (800 mL) under vigorous stirring at room temperature. An $NaBH_4$ solution (2 g, 53 mmol) in ammonia (3.5%, 100 mL) was then quickly added to the mixture. Soon after the occurrence of the reduction reaction, the temperature of the system was increased to 100°C and kept constant for 2 hours. The material was cooled at room temperature and aged in water for another 12 hours. This product was separated by the imposition of an external magnet and washed several times with water. This material was transformed into a red-brown powder (final synthesis product) by drying and curing at 400°C for 2 hours. The resulting nanopowder showed a magnetic response upon exposure to a magnetic field. The final mass of the product was 2.0 g (12.5 mmol) of Fe_2O_3 and a yield of 68% was calculated.

The resulting nanoparticulated material was characterized by zero field and in field (5T) Mossbauer spectroscopy, FTIR spectroscopy, high-resolution TEM, X-ray powder diffraction, magnetization measurements,[11,12] and constituted stoichiometric maghemite (γ-Fe_2O_3) with a mean diameter of 10 ± 2 nm. Sonication in water (mod. 221, 48 kHz, 50 W; Branson Ultrasonic Corporation, Danbury, CT) can form a stable colloidal suspension without any organic or inorganic coverage. Notwithstanding, the surface of these bare maghemite nanoparticles shows peculiar binding properties and can be reversibly derivatized with selected organic molecules. These bare nanoparticles are called surface-active maghemite nanoparticles (SAMNs).

Preparation of rhodamine bound nanoparticles

The surface of bare SAMNs can be superficially and reversibly derivatized by simple incubation in 50 mM tetramethylammonium perchlorate, pH 7.0, in the presence of 50 μM RITC. The amount of bound RITC was calculated from the disappearance of the RITC absorbance at 554 nm in the supernatant ($\varepsilon = 6.6 \times 10^4\,M^{-1}cm^{-1}$). Following the application of an external magnet, SAMN–RITC suspensions were extensively washed in 50 mM tetramethylammonium perchlorate and no leaching of the rhodamine derivative was evident, as determined by absorbance spectroscopy of the resulting supernatant upon external magnet application. The resulting fluorescent magnetic nanoparticles were comprised of 29.1 ± 3.8 μmol RITC per g of SAMNs.

Preparation of bovine serum amine oxidase adduct with rhodamine-modified maghemite nanoparticles

RITC can be used as a spacer-arm and presents the isothiocyanate functionality to which the primary amino groups of selected molecules can be covalently linked. In this way, a magnetically drivable fluorescent nanocarrier was prepared using the SAMN–RITC adduct. In the present work, the binding reaction was performed by adding 11 μM BSAO in 0.1 M KCl containing 5 g L⁻¹ SAMN-RITC nanoparticles and stirring overnight at 4°C. The unbound enzyme was removed with the aid of an external magnet application using extensive nanoparticle washing.

Determination of nanoparticle bound amine oxidase by mass spectrometry

The nature and optical scattering properties of maghemite nanoparticles interferes with the determination of proteins bound on their surface by the classical protein determination methods. To overcome this limitation, an alternative approach based on protein quantitation by mass spectrometry was applied.

BSAO samples, native or nanoparticle bound, were extensively dialyzed against 40 mM ammonium bicarbonate (3 × 2 hour buffer changes with a 1000:1 volume ratio),

dried under a vacuum, and resuspended in 100 µL of 40 mM ammonium bicarbonate. Native and SAMN-bound BSAO samples were normalized based on their enzymatic activity and incubated overnight at 37°C with sequencing grade trypsin (Promega, Madison, WI) and an enzyme to substrate ratio of 120 (w/w, based on specific activity of the native BSAO). After tryptic digestion, samples were centrifuged at 14000× g for 10 minutes and exposed to an external magnet for 30 minutes to remove SAMN. Finally, the supernatant were dried under a vacuum, dissolved in 20 µL of 0.1% formic acid, and analyzed by liquid chromatography coupled with tandem mass spectrometry (LC-MS/MS) using a 6520 Q-TOF mass spectrometer, which was coupled on-line with a 1200 series high-pressure liquid chromatography system through a Chip Cube Interface (Agilent Technologies, CA). Each sample (4 µL) was loaded onto a C18 large capacity chip-column that integrated a 160 nL capacity trap-column, an RP column (75 µm × 150 mm), connection capillaries, and a nanospray emitter. Solvent A was water/formic acid 0.1% and solvent B was acetonitrile/formic acid 0.1%. Peptides were separated with a linear gradient of 0%–50% of solvent B in 50 minutes at a flow rate of 0.3 µL min^{-1}. Mass spectra were acquired in a data-dependent mode; tandem mass spectra of the four most intense ions were acquired for each MS scan, which ranged from 350–3000 Da. The scan speed was set to 2 MS spectra s^{-1} and 2 MS/MS spectra s^{-1}. Capillary voltage was set to 1850 V and drying gas to 5 L s^{-1}. Raw data files were converted into Mascot generic format (MGF) files using MassHunter Qualitative analysis software (Agilent Technologies, Santa Clara, CA). MGF files were analyzed using Mascot Search Engine server version 2.3 (Matrix Science, London, UK). Spectra were searched against the SwissProt database (May 2011 version, Taxonomy Mammalia, 65453 entries) with the following parameters: enzyme specificity was set to trypsin with up to two missed cleavages, and peptide and fragment tolerance were set to 6 ppm and 0.05 Da, respectively. Oxidation of methionine was selected as a modification variable. Based on the search against the corresponding randomized database, false discovery rates (FDR) of 0.1% were calculated. Only identified peptides with a confidence of ≥99% were used to quantify the amount of BSAO bound to nanoparticles.

Enzyme activity measurements

A spectrophotometric assay was used to measure the activity of amine oxidase free in solution and immobilized on SAMNs. Initial rate measurements were carried out according to the peroxidase-coupled assay reported by Stevanato et al.[29] The H$_2$O$_2$ produced during spermine oxidation was continuously monitored by the change of absorbance at 555 nm, under continuous stirring, using an extinction coefficient, ε, of 2.2×10^4 M^{-1}cm^{-1}. Unless otherwise specified, all experiments were carried out in air-saturated solutions of 20 mM HEPES (4-(2-hydroxyethyl)-1-piperazine-ethanesulfonic acid), pH 7.5, at room temperature (22°C ± 1°C) in the presence of 0.1 mM EDTA. Protein concentration was measured according to the Bradford method,[30] which uses bovine serum albumin as a standard.

Data analysis

Catalytic constant (k$_c$) and catalytic efficiency (k$_c$/K$_M$) were calculated from the V$_{max}$ and K$_M$ values and were obtained by nonlinear best fit of experimental data on Michaelis–Menten equation and by assuming a BSAO molecular mass of 170 kDa.[31]

Experimental data were fitted using the Sigma Plot program (v. 10.0; Jandel Scientific, San Rafael, CA).

Results
Nanoparticles resuspension in different media

In order to characterize the nanoparticle's surface, stable colloidal water suspensions are a necessity. In the present case, maghemite nanoparticles were synthesized according to an innovative method[11,12] and suspended in bidistilled water using an ultrasonic bath (mod. 221 at 48 kHz, 50 W; Bransonic). Upon ultrasound application, suspensions were sampled and the absorbance was read every 30 minutes. It was found that, by measuring the increase of suspension absorbance during sonication, the dispersion exhibited exponential behavior. As previously described, the first order kinetic constants were in the range 10–100 mg L^{-1} and independent of the nanoparticles' concentration.[12] In water, the dispersion kinetic constant resulted in 0.85 ± 0.055 h^{-1}. The colloidal suspension of maghemite nanoparticles was stable for more than 6 months without precipitation or aggregation phenomena.

Beside SAMN stability in water, the biotechnological applications of magnetic nanoparticles are supposed to be carried out in buffered solutions. According to previous research on the stabilizing/destabilizing effects of different cations and anions on iron oxide nanoparticle suspensions,[32] the dispersion process of our bare SAMNs was carried out in 50 mM tetramethylammonium perchlorate. Under these conditions, colloidal SAMN dispersions were stable and further experiments on the dispersion process of SAMN were performed using the same experimental conditions.

RITC binding to nanoparticle surface

Preliminary experiments showed that the SAMN surface is able to selectively interact with different organic molecules and enzymes. For example, SAMNs are able to interact directly with avidin, but not with bovine serum amine oxidase. This suggests some kind of recognition process between SAMN surface and protein molecules, which will be explored elsewhere.

In order to improve our knowledge of maghemite nanoparticles' surface properties, various fluorescent dyes, characterized by similar structures and different functional groups, were tested (Figure 1).

Maghemite nanoparticles (100 mg L^{-1}) were dispersed in 50 mM tetramethylammonium perchlorate, pH 7.0, and were incubated with the fluorescent probe (10 µM). The test tube was gently shaken for one hour at room temperature. After the incubation period, nanoparticles were separated using an external magnetic field. The supernatant was checked at the maximum absorbance wavelength of the probe, as reported in Table 1.[33]

A significant fluorophore absorbance reduction was measured only when nanoparticles were incubated in the presence of RITC. No reduction of the absorbance was detected with other fluorescent probes. This suggests that only RITC is able to bind to the nanoparticle's surface. This indicates that the coexistence of isothiocyanate and an amino group on the molecule is necessary to anchor the molecule to the surface of the SAMN.

The binding phenomenon between maghemite nanoparticles and RITC is completed within a few minutes and forms a stable suspension of the fluorescent magnetic complex.

RITC binding on maghemite surface was determined as a function of fluorescent probe concentration, in the range 10–100 µM, in 50 mM tetramethylammonium perchlorate, at pH 7. RITC concentrations above 100 µM were not considered because the probe is not soluble above this concentration. In the concentration range explored, the amount of the bound probe on the nanoparticle's surface depended on its concentration in the solution. Experimental data were analyzed according to the Langmuir isotherm model[34] and the maximum-loading capacity, q_{max}, was 0.14 mg RITC mg^{-1} SAMN. A Langmuir binding constant, K_L, of 61.7 mL mg^{-1} was calculated. The result corresponded to 533 RITC molecules per nanoparticle.

After washing and freeze-drying, the adduct formed with maghemite nanoparticles and RITC (SAMN–RITC) was studied using FTIR spectroscopy. In Figure 2, the FTIR spectra of the SAMN–RITC complex, as well as that of the maghemite nanoparticle and the free RITC, are reported. As shown in the figure, the comparison between the spectra of the free RITC and of the SAMN–RITC complex showed the relevant broadening of FTIR bands at 1412 cm^{-1}, which is attributable to CH_2 bending of $-N-(CH_2-CH_3)_2$ groups,[35] inset of Figure 2. Furthermore, the disappearance of the FTIR band at 2030–2150 cm^{-1} was observed and attributed to the isothiocyanate group.[36] In contrast with the other probes
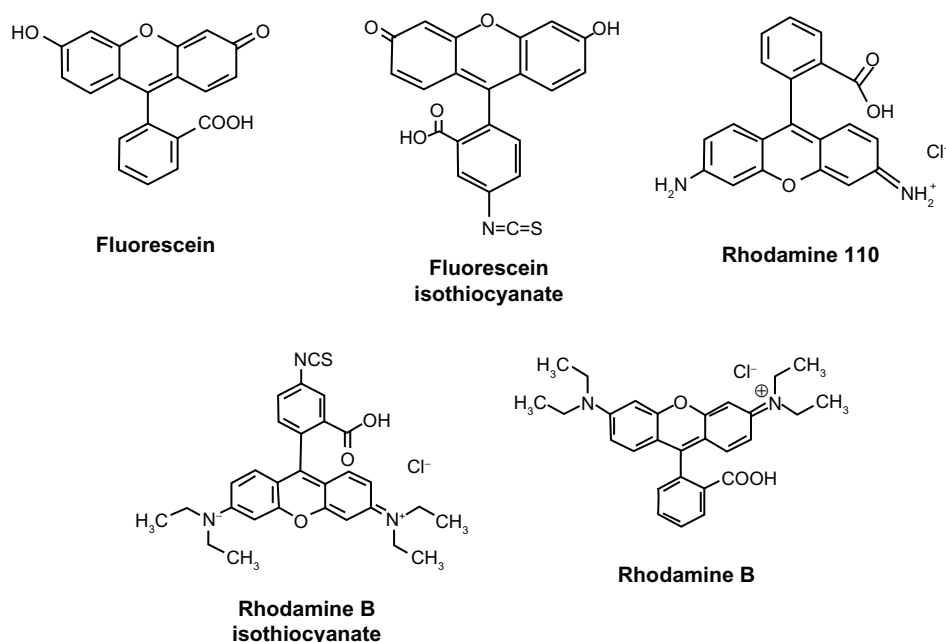

Figure 1 Structures of the fluorescent dyes used as probes for nanoparticle surface properties.

Table 1 Optical characteristics of fluorescent dyes used to test maghemite nanoparticle surface properties

Fluorescent probe	Molar extinction coefficient (m⁻¹cm⁻¹)	Excitation wavelength (nm)	Emission wavelength (nm)	Quantum yield[a]
Fluorescein	65,000	494	520	0.79
Fluorescein isothiocyanate	65,000	494	520	0.79
Rhodamine B	106,000	554	580	0.49
Rhodamine B isothiocyanate	106,000	554	580	0.49
Rhodamine 110	90,000	498	520	0.9

Note: [a]The quantum yield was determined in ethanol.[33]

tested, this suggests the involvement of the −N=C=S moiety in the binding and confirms its responsibility in specific interaction with RITC.

SAMN–RITC was compared with free rhodamine and the fluorescence characteristics were determined. The SAMN–RITC complex is fluorescent and shows an excitation and emission spectra similar to unbound RITC. With respect to the free fluorophore, a quantum yield of 8.9% ± 1.3% was estimated for the immobilized RITC, which is sufficient to apply the developed material as a magnetic fluorescent probe.

In order to improve our knowledge about the binding properties of RITC on SAMN's surface, it has been observed that the pH was fundamentally important in regulating the amount of adsorbed molecules. We have tested SAMN's capability in binding RITC in the pH range 2–10 in 50 mM tetramethylammonium perchlorate. The results in Figure 3 show that the phenomenon is well described by a sigmoidal behavior. This suggests the existence of two different binding modalities, in acidic and basic pH extremities, respectively. In particular, we observed that the ability of RITC to interact with nanoparticles increases at acidic pH values. The amount of bound RITC at pH 4.0 was about 500 molecules per nanoparticle and the amount of bound RITC at basic pH values (pH 10.0) decreases to about 150 molecules per nanoparticle.

These data offer a new perspective about the behavior of RITC adsorption on SAMN surface that involves not only electrostatic interactions. In fact, at acidic pH, we observed the highest amount of bound molecules per nanoparticle. From a purely electrostatic point of view, we should observe a repulsive interaction between RITC and SAMN surface, because both the species are protonated at low pH.

The complexing ability of thiocyanate and isothiocyanate group toward iron(III) is well known. In order to obtain further information on the influence of the isothiocyanate group on the binding phenomenon, we prepared three different RITC
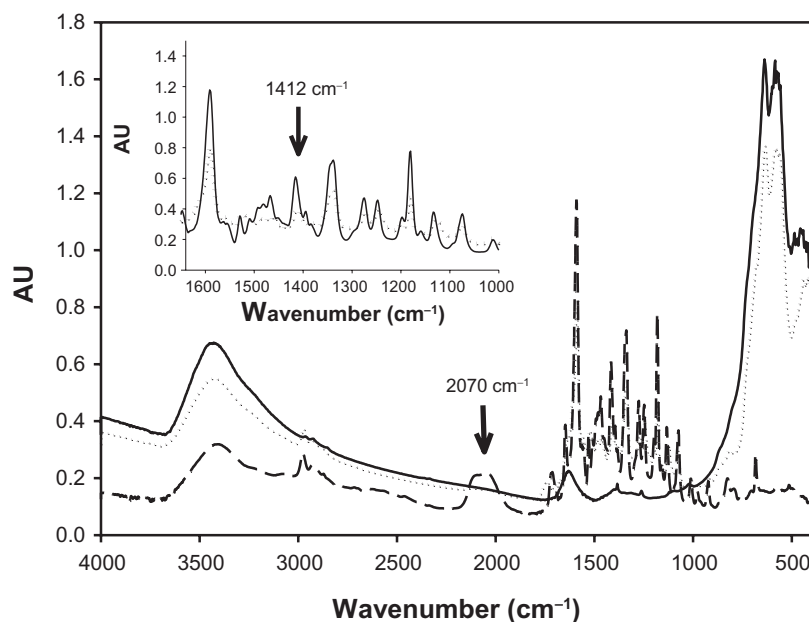

Figure 2 FTIR spectra of bare maghemite nanoparticles, rhodamine B isothiocyanate and SAMN–RITC complex. Samples were lyophilized, homogenized with KBr powder, and pelleted by an 8.0 ton hydraulic press. (—) SAMN, (---) RITC; (········) SAMN–RITC. **Inset:** Comparison of FTIR spectra of RITC and SAMN–RITC complex in the region 1365–1000 cm⁻¹. (—), RITC; (········), SAMN–RITC.
Abbreviations: SAMN, surface-active maghemite nanoparticles; RITC, rhodamine B isothiocyanate; KBr, potassium bromide; FTIR, Fourier-transform infrared.
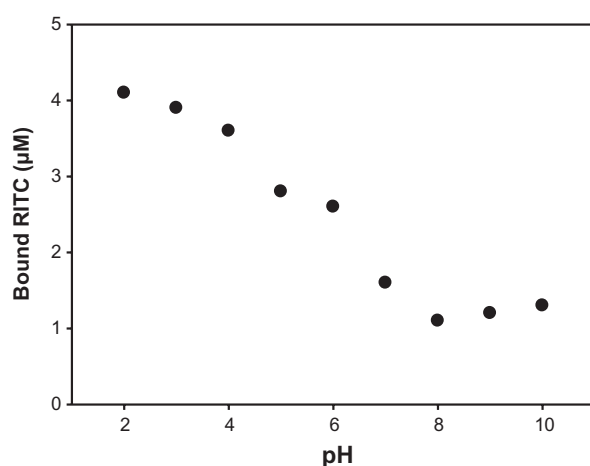
Figure 3 RITC binding to maghemite nanoparticle surface as a function of pH.
Note: Experiments were carried out in 50 mM tetramethylammonium perchlorate in the presence of 10 μM RITC and 100 mg L^{-1} SAMN, measuring the decrease of solution absorbance at 554 nm.
Abbreviations: SAMN, surface-active maghemite nanoparticles; RITC, rhodamine B isothiocyanate.

Table 2 Binding of RITC derivatives to bare maghemite nanoparticles

RITC-derivative	Number of bound μmol RITC per g nanoparticle	
	Experimental conditions	
	pH 7.0	pH 10.0
None	2.5	1
—NH—CH$_2$—NH$_2$	2	5
—NH—CH$_2$—CH$_2$—COOH	11	7
—NH—CH$_2$—CH$_2$—OH	17	12

Note: The binding process was carried out in 50 mM tetramethylammonium perchlorate in the presence of 100 mg/L maghemite nanoparticles.

derivatives (Table 2) formed by the condensation of different primary amines to the isothiocyanate group of the fluorescent probe, namely ethylenediamine, glycine, and 2-aminoethanol, and characterized by differently functional terminal groups. As shown in Table 2, the best binding properties were evidenced by the ethanolamine-RITC derivative, both at pH 7.0 and at pH 10.0. Possibly due to the chelating properties of —COOH, —OH, and —NH$_2$, all three RITC derivatives that are used provide an anchoring function with respect to under coordinated iron sites on the nanoparticle's surface.[37]

It should be noted that the role of hydrophobic interactions between the RITC and nanoparticles was studied in the presence of a surfactant (0.1% sodium dodecylsulfate) and no variation of the binding process was noted and there was no evidence of hydrophobic interaction (data not shown).

Surface coating of maghemite nanoparticles with RITC and bovine serum amine oxidase

BSAO is a copper enzyme with a molar weight of approximately 170 kDa.[31] It is a redox-protein that oxidatively deaminates polyamines containing primary amine groups (putrescine, spermidine and spermine) with the concomitant production of hydrogen peroxide, the corresponding aldehydes, and ammonia.[17,24]

Preliminary experiments showed that BSAO cannot bind directly on the surface of SAMNs. Thus, in order to immobilize BSAO on SAMNs surface, RITC was used as a spacer-arm. This presents the isothiocyanate functionality

to which primary amino groups of the enzyme molecule can be covalently linked.

The binding reaction was performed by adding 11 μM BSAO in 0.1 M KCl, pH 7.0, to a suspension containing 5 g L^{-1} SAMN, which were previously covered by 29.1 μmol RITC g^{-1} SAMN. The solution was stirred overnight at 4°C. The unbound enzyme was removed by repeated nanoparticle washing cycles with the aid of an external magnetic field. After three washing cycles, the activity of the immobilized enzyme was constant and no detectable enzyme release was observed in the solution. The enzyme-bound nanoparticles could be used for the preparation of magnetically recoverable fluorescent nanocatalyst.

Transmission electron micrographs show the coating of BSAO on SAMN–RITC, which forms a less electron-dense shell that covers the iron oxide nanoparticles. The average shell thickness ranges from 6–8 nm (Figure 4).
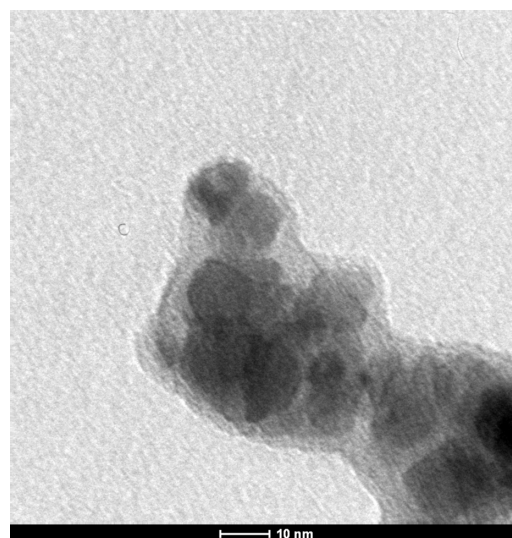

Figure 4 TEM image of maghemite nanoparticles derivatized with RITC and with immobilized BSAO (SAMN–RITC–BSAO).
Abbreviations: BSAO, bovine serum copper-containing amine oxidase; SAMN, surface-active maghemite nanoparticles; RITC, rhodamine B isothiocyanate; TEM, transmission electron microscopy.

By comparing the trypsin digestion of native and bound enzymes, the amount of immobilized BSAO on SAMNs was determined by mass spectrometry and characterized by the same enzymatic activity, as reported in the Materials and methods section of this research. The digestion yielded 42% sequence coverage between the two samples (Figure 5). The ten most abundant common peptides, characterized by a score >35 ($P < 0.01$) and accounting for about 22% of the sequence coverage, were quantitatively compared to calculate the specific activity of bound BSAO (Table 3). The aggregate signal of the ten peptides from maghemite-bound BSAO was 2.85 times higher than the aggregate signal of the EIC from the free protein with the same activity.

After immobilization, enzyme activity was calculated by measuring the rate of amine oxidase-catalyzed oxidation of spermine. The initial reaction rate was measured as a function of substrate concentration determining the hydrogen peroxide production in the presence of free or immobilized enzymes. Measurements of immobilized enzyme activity were performed by stirring. Under our experimental conditions, the reaction rate was independent of the stirring rate. This indicates that the kinetic of the reaction is not diffusion-controlled. Table 4 shows the kinetic parameters obtained by measuring the activity of native and immobilized BSAO. In the case of nanoparticles without rhodamine coating, no enzyme activity

associated with nanoparticles was detected. The comparison of the enzymatic activity of BSAO bound to SAMN–RITC or free in solution, under the same experimental conditions, indicates that BSAO was successfully immobilized on the magnetically drivable fluorescent SAMN, displaying detectable catalytic activity on spermine (k_c = 14.4 min^{-1}). Immobilized BSAO shows a catalytic constant of about 30% of the value shown by native BSAO, corresponding to 0.81 IU g^{-1} SAMN. The value of the enzyme Michaelis constant, K_M, was almost doubled upon binding. Correspondingly, the binding process led to a sixfold decrease of the BSAO catalytic efficiency, k_c/K_M.

The system SAMN–RITC–BSAO was removed from the solution by application of an external magnet. Monitoring the disappearance of fluorescence from the assay solution and activity measurements were repeated. This shows that SAMN–RITC–BSAO maintains its catalytic activity over repeated washing cycles.

Discussion

In order to test bare maghemite surface properties, we utilized different fluorescent probes. Among the probes reported in Figure 1, only RITC was able to bind to the nanoparticle surface. The comparison of fluorophore molecule structures indicates that multiple possible interaction sites belonging to RITC could interact with the surface of maghemite

```
  1 MFIFIFLSLW TLLVMGREEG GVGSEEGVGK QCHPSLPPRC PSRSPSDQPW
 51 THPDQSQLFA DLSREELTTV MSFLTQQLGP DLVDAAQARP SDNCVFSVEL
101 QLPPKAAALA HLDRGSPPPA REALAIVFFG GQPQPNVTEL VVGPLPQPSY
151 MRDVTVERHG GPLPYYRRPV LLREYLDIDQ MIFNRELPQA AGVLHHCCSY
201 KQGGQKLLTM NSAPRGVQSG DRSTWFGIYY NITKGGPYLH PVGLELLVDH
251 KALDPADWTV QKVFFQGRYY ENLAQLEEQF EAGQVNVVVI PDDGTGGFWS
301 LKSQVPPGPT PPLQFHPQGP RFSVQGNRVA SSLWTFSFGL GAFSGPRVFD
351 VRFQGERLAY EISLQEAGAV YGGNTPAAML TRYMDSGFGM GYFATPLIRG
401 VDCPYLATYM DWHFVVESQT PKTLHDAFCV FEQNKGLPLR RHHSDFLSHY
451 FGGVAQTVLV FRSVSTMLNY DYVWDMVFYP NGAIEVKLHA TGYISSAFLF
501 GAARRYGNQV GEHTLGPVHT HSAHYKVDLD VGGLENWVWA EDMAFVPTAI
551 PWSPEHQIQR LQVTRKQLET EEQAAFPLGG ASPRYLYLAS KQSNKWGHPR
601 GYRIQTVSFA GGPMPQNSPM ERAFSWGRYQ LAITQRKETE PSSSSVFNQN
651 DPWTPTVDFS DFINNETIAG KDLVAWVTAG FLHIPHAEDI PNTVTVGNGV
701 GFFLRPYNFF DQEPSMDSAD SIYFREGQDA GSCEINPLAC LPQAATCAPD
751 LPVFSHGGYP EY
```

Figure 5 Amino acid sequence coverage of native and bound BSAO.
Notes: Bold letters indicate amino acid total sequence coverage (42%) obtained after trypsin digestion and analysis by MS/MS mass spectrometry of nanoparticle-bound BSAO. Underscore, bold letters indicate the amino acid sequences that were used for relative quantification of nanoparticle-bound BSAO.
Abbreviations: BSAO, bovine serum copper-containing amine oxidase; MS/MS, tandem mass spectroscopy.

Table 3 The ten most abundant 10 common peptides obtained after trypsin digestion of native and SAMN bound BSAO

Peptide number	Score	Bound BSAO	Native BSAO	Bound/free
1. YLYLASK	36	747655	132977	
2. ALDPADWTVQK	67	7693036	10761424	
3. GGPYLHPVGLELLVDHK	55	11988500	17391553	
4. YMDSGFGMGYFATPLIR	101	9442405	4823422	
5. ALDPADWTVQKVFFQGR	44	1239335	539496	
6. KQLETEEQAAFPLGGASPR	87	13640798	9686214	
7. SQVPPGPTPPLQFHPQGPR	63	113110365	15533939	
8. IQTVSFAGGPMPQNSPMER	132	44140030	11272321	
9. LAYEISLQEAGAVYGGNTPAAMLTR	169	3758314	1981715	
10. HHSDFLSHYFGGVAQTVLVFR	41	4856416	1648758	
Sum		210616854	73771819	2.85

nanoparticles. A possible interaction with the carboxyl groups was studied by comparing the behavior of fluorescein probe in 50 mM tetramethylammonium perchlorate, as suggested in the literature.[38] At neutral pH, the carboxyl group is negatively charged. The probe was incubated with nanoparticles as illustrated above. In this case, no binding was observed. This suggests that the probe, at pH 7.0, did not interact with the nanoparticle surface. It can also be deduced that the carboxyl group is not involved in the binding of RITC.

The adduct formed with maghemite nanoparticles and RITC (SAMN–RITC), after washing and freeze-drying, was studied by FTIR spectroscopy. It is known that the major absorption bands of iron oxides locate in the region 400–800 cm^{-1} (Figure 2). In this case, the distinctive features of maghemite (bands at 445 and 630 cm^{-1}) indicate cation vacancies.[39,40] Furthermore, the comparison between the spectra of free RITC and of SAMN–RITC shows absorption bands at 2030–2150, 1589, 1412, 1345, 1274, 1249, and 1180 cm^{-1} (Figure 2). These bands are attributable to the isothiocyanate group, the stretching vibrational mode of C=C in benzene rings, the bending vibration of CH$_2$ in $-$N$-$(C$_2$H$_5$)$_2$, the vibration of C$-$N-linked benzene ring, the vibration of C$-$O of COOH, the vibration of C-N in $-$N$-$(C$_2$H$_5$)$_2$ group, and the asymmetric stretch vibration of C$-$O$-$C, respectively.[35] No apparent changes were found in absorption bands at 1589, 1345, 1274, 1249, and 1180 cm^{-1}. Conversely, the relevant broadening of FTIR vibration at 1412 cm^{-1}, attributable to CH$_2$ bending of $-$N$-$(C$_2$H$_5$)$_2$ groups (inset of Figure 2) and the disappearance of the FTIR band at

2030–2150 cm^{-1}, is attributable to the isothiocyanate group. This suggests the involvement of these functionalities in the binding. These results suggest a multiple point binding that involves, in addition to the $-$S=C=N functionality, the tertiary amino groups of the RITC xanthene condensed rings. This is in contrast to the other probes tested that do not contain these two functionalities at the same time. Thus, the presence of the $-$S=C=N moiety on the fluorescent molecule had a positive effect on nanoparticle binding. Nevertheless, this chemical functionality is not sufficient to guarantee a stable adduct formation, as observed by incubating SAMN with fluorescein isothiocyanate. The tertiary amino groups of the RITC xanthene condensed rings, as indicated by the broadening of the FTIR band at 1412 cm^{-1}, are not able to guarantee a stable adduct formation without the concomitant participation of isothiocyanate, as demonstrated by experiments with rhodamine B. In order to verify the involvement of the isothiocyanate group already evidenced by FTIR spectroscopy, three different amines have been bound to RITC (glycine, ethylene-diamine, and ethanolamine). Modified RITC molecules have been incubated with nanoparticles in 50 mM tetramethylammonium perchlorate and tested at pH 7.0 and 10.0. The amount of modified RITC molecules interacting with nanoparticles depends on the modification of the isothiocyanate group. This influences the ability of the fluorescent probe to interact with the nanoparticle's surface and confirms the role of the isothiocyanate group in the binding, even if modified as a thiorurea.

The peculiarities of RITC allow the interaction with maghemite nanoparticle surface and the formation of a stable adduct (SAMN–RITC). This magnetic nanomaterial adduct was stable across a wide pH range, even if the number of RITC molecules bound to the surface of SAMN was dependent on pH.

Exploiting the chemical properties of the isothiocyanate functionality, this paper describes the surface modification of BSAO that was covalently bound to RITC to develop a

Table 4 Kinetic parameters of native and SAMN-bound BSAO

Enzyme form	Kinetic parameters		
	K$_M$ (μM)	k$_c$ (min^{-1})	k$_c$/K$_M$ (μM^{-1} min^{-1})
Native BSAO	7.4	46.8	6.3
SAMN–RITC–BSAO	14.0	14.4	1.0

Abbreviations: BSAO, bovine serum copper-containing amine oxidase; SAMN, surface-active maghemite nanoparticles; RITC, rhodamine B isothiocyanate.

magnetically controllable rhodamine-based nanocatalyst. The immobilization, as a monomolecular layer, allows an improved performance of the enzyme by retaining its catalytic activity towards the oxidation of spermine for more than ten days. In tumor cells, the prepared fluorescent magnetically drivable nanocatalyst could be easily used to produce cytotoxic products, hydrogen peroxide, and aldehydes, due to the high concentration of endogenous polyamines (spermine or spermidine) or, alternatively, to remove spermine and other BSAO substrates from aqueous solutions. The presence of the nanocatalyst can be conveniently monitored by its fluorescence. Moreover, the nanocatalyst can be quickly removed by the application of an external magnet and re-used without loss of the catalytic efficiency. The results demonstrate that the polyamine-degrading enzyme BSAO is a very good candidate to develop a magnetic fluorescent adduct. These results can be used in further investigations of BASO's therapeutic potential in mice-bearing tumors of various human origins. We expect that these studies will suggest new strategies to potentiate the killing of cancer cells using BSAO, which might be essential for discovering a novel anticancer therapy.

Magnetic nanomaterials are generally used as theranostic tools as drug carriers, in hyperthermia treatment, or as contrast agent in MRI.[41,42]

The novelty of the present approach is represented by the possibility to drive the catalytic activity of an enzyme, BSAO, with an easily magnetically removable, fluorescent-detectable nanocomposite that is able to transform enzymatic products into cytotoxic molecules in tumor cells. The advantages of this new strategy are its high specificity due to enzyme substrate accumulation in tumor cells, the ease of detectability by fluorescence imaging and targeting, and removability by magnetic field application.

Alternatively, the SAMN–RITC–BSAO adduct could be used as a magnetically drivable nanoreactor to reduce polyamine content of common foodstuffs in an attempt to reduce the polyamine intake in cancer patients. As previously shown by Bardocz et al,[43] some food ingredients contain large quantities of polyamines and preliminary clinical trials performed in metastatic hormone-refractory prostate cancer patients have revealed the feasibility of a nutrition therapy based upon a 6-month polyamine-reduced diet.[44,45]

In conclusion, it is worth pointing out that the production process is very cheap and, by not involving organic solvents surfactants or particular capping strategies, it can be considered a "green chemistry" product. Nevertheless, the favorable magnetic properties of the material are guaranteed by optimizing the magnetic material/organic shell ratio.

Acknowledgments

Disclosure

The authors report no conflicts of interest in this work.

References

1. Selvan ST, Hayakawa T, Nogami M, et al. Sol-gel derived gold nanoclusters in silica glass possessing large optical nonlinearities. *J Phys Chem B*. 2002;106(39):10157–10162.
2. Palecek E, Fojta M. Magnetic beads as versatile tools for electrochemical DNA and protein biosensing. *Talanta*. 2007;74(3):276–290.
3. Ravindranath SP, Mauer LJ, Deb-Roy C, Irudayaraj J. Biofunctionalized magnetic nanoparticle integrated mid-infrared pathogen sensor for food matrixes. *Anal Chem*. 2009;81(8):2840–2846.
4. Chen WJ, Tsai PJ, Chen YC. Functional nanoparticle-based proteomic strategies for characterization of pathogenic bacteria. *Anal Chem*. 2008;80(24):9612–9621.
5. Taylor JI, Hurst CD, Davies MJ, Sachsinger N, Bruce IJ. Application of magnetite and silica-magnetite composites to the isolation of genomic DNA. *J Chromatogr A*. 2000;890(1):159–166.
6. Yang HH, Zhang SQ, Chen XL, Zhuang ZX, Xu JG, Wang XR. Magnetite-containing spherical silica nanoparticles for biocatalysis and bioseparations. *Anal Chem*. 2004;76(5):1316–1321.
7. Ito A, Shinkai M, Honda H, Kobayashi T. Medical application of functionalized magnetic nanoparticles. *J Biosci Bioeng*. 2005;100(1): 1–11.
8. Tanaka T, Matsunaga T. Fully automated chemiluminescence immunoassay of insulin using antibody-protein A-bacterial magnetic particle complexes. *Anal Chem*. 2000;72(15):3518–3522.
9. Neuberger T, Schopf B, Hofmann H, Hofmann M, Rechenberg BV. Superparamagnetic nanoparticles for biomedical applications: possibilities and limitations of a new drug delivery system. *J Magn Magn Mater*. 2005;293(1):483–496.
10. Liu Z, Liu Y, Yang H, Yang Y, Shen G, Yu R. A phenol biosensor based on immobilizing tyrosinase to modified core-shell magnetic nanoparticles supported at a carbon paste electrode. *Anal Chim Acta*. 2005;533(1):3–9.
11. Magro M, Valle G, Russo U, Nodari L, Vianello F, inventors; University of Padua, Magro M, Valle G, Vianello F. assignees. Maghemite nanoparticles and method for preparing thereof. European patent PCT/EP2010/060486. July 15, 2010.
12. Magro M, Sinigaglia G, Nodari L, et al. Charge binding of rhodamine derivative to OH⁻ stabilized nanomaghemite: Universal nanocarrier for construction of magnetofluorescent biosensors. *Acta Biomaterialia*. 2012 Feb 13 [Epub ahead of print]. Available from: http://dx.doi.org/10.1016/j.actbio.2012.02.005. Accessed 20 April, 2012.
13. Knowles PF, Dooley DM. Amine oxidases. In: Sigel H, Sigel A, editors. *Metal Ions in Biological Systems*. New York, NY: Marcel Dekker; 1994:361–403.

14. Casero RA Jr, Pegg AE. Polyamine catabolism and disease. *Biochem J*. 2010;421(3):323–338.

15. Janes SM, Klinman JP. An investigation of bovine serum amine oxidase active site stoichiometry: evidence for an aminotransferase mechanism involving two carbonyl cofactors per enzyme dimer. *Biochemistry*. 1991;30(18):4599–4605.

16. Cai DY, Klinmann JP. Evidence for a self-catalytic mechanism of 2,4,5-trihydroxyphenylalanine quinone biogenesis in yeast copper amine oxidase. *J Biol Chem*. 1994;269(51):32039–32042.

17. Mondovì B, Riccio P, Agostinelli E, Marcozzi G. Oxidation of diamines and polyamines. In: Bachrach U, Heimer YM, editors. *The Physiology of Polyamines*. Vol 1. Boca Raton, FL: CRC Press; 1989:177–201.

18. Bachrach U. Polyamines as indicators of disease activity and response to therapy in cancer patients. In: Bachrach U, Heimer YM, editors. *The Physiology of Polyamines*. Vol 2. Boca Raton, FL: CRC Press; 1989:234–249.

19. Agostinelli E, Tempera G, Molinari A, et al. The physiological role of biogenic amines redox reactions in mitochondria. New perspective in cancer therapy. *Amino Acids*. 2007;33(2):175–187.

20. Lindsay GS, Wallace HM. Changes in polyamine catabolism in HL-60 human promyelogenous leukaemic cells in response to etoposide-induced apoptosis. *Biochem J*. 1999;337(Pt 1):83–87.

21. Calcabrini A, Arancia G, Marra M, et al. Enzymatic oxidation product of spermine induce greater cytotoxic effects on human multidrug-resistant colon carcinoma cells (LoVo) than on their wild-type counterparts. *Int J Cancer*. 2002;99(1):43–52.

22. Averill-Bates DA, Cherif A, Agostinelli E, Tanel A, Fortier G. Anti-tumoral effect of native and immobilized bovine serum amine oxidase in a mouse melanoma model. *Biochem Pharmacol*. 2005;69(12):1693–1704.

23. Agostinelli E, Seiler N. Non-irradiation-derived reactive oxygen species (ROS) and cancer. Therapeutic implications. *Amino Acids*. 2006;31(3):341–355.

24. Agostinelli E, Belli F, Molinari A, et al. Toxicity of enzymatic oxidation products of spermine to human melanoma cells (M14): sensitization by heat and MDL 72527. *Biochim Biophys Acta*. 2006;1763(10):1040–1050.

25. Agostinelli E, Belli F, Dalla Vedova L, Marra M, Crateri P, Arancia G. Hyperthermia enhances cytotoxicity of amine oxidase and spermine on drug-resistant colon adenocarcinoma cells (LoVo). *Int J Oncol*. 2006;28(6):1543–1553.

26. Agostinelli E, Dalla Vedova L, Belli F, Condello M, Arancia G, Seiler N. Sensitization of human colon adenocarcinoma cells (LoVo) to reactive oxygen species by lysosomotropic compounds. *Int J Oncol*. 2006;29(4):947–955.

27. Agostinelli E, Arancia G, Dalla Vedova L, et al. The biological functions of polyamine oxidation products by amine oxidases: perspectives of clinical applications. *Amino Acids*. 2004;27(3–4):347–358.

28. Turini P, Sabatini S, Befani O, et al. Purification of serum amine oxidase. *Anal Biochem*. 1982;125(2):294–298.

29. Stevanato R, Mondovì B, Sabatini S, Rigo A. Spectrophotometric assay for total polyamines by immobilized amine oxidases. *Anal Chim Acta*. 1990;237:391–397.

30. Bradford MM. A rapid and sensitive method for the quantitation of microgram quantities of protein utilizing the principle of protein-dye binding. *Anal Biochem*. 1976;72:248–254.

31. Bellelli A, Morpurgo L, Mondovì B, Agostinelli E. The oxidation and reduction reactions of bovine serum amine oxidase. a kinetic study. *Eur J Biochem*. 2000;267(11):3264–3269.

32. Lucas T, Dubois E, Chevalet J, Durand-Vidal S, Joiret S. Reactivity of nanocolloidal particles γ-Fe_2O_3 at charged interfaces. Part 2. Electrochemical conversion. Role of the electrode material. *Phys Chem Chem Phys*. 2008;10(22):3274–3286.

33. Valeur B. *Molecular Fluorescence: Principles and Applications*. Weinheim, Germany: Wiley-VHC; 2002.

34. Hung CW, Holoman TRP, Kofinas P, Bentley WE. Towards oriented assembly of proteins onto magnetic nanoparticles. *Biochem Eng J*. 2008;38:164–170.

35. Liu X, Cui D, Wang Q, Xu H, Li M. Photoluminescence enhancement of ZrO2/rhodamine B nanocomposite. *J Mat Sci*. 2005;40(5):1111–1114.

36. Vieira Ferreira LF, Cabral PV, Almeida P, Oliveira AS, Reis MJ, Botelho do Rego AM. Ultraviolet/visible absorption, luminescence, and X-ray photoelectron spectroscopic studies of a rhodamine dye covalently bound to microcrystalline cellulose. *Macromolecules*. 1998;31(12):3936–3944.

37. Chen LX, Liu, T, Thurnauer MC, Csencsits R, Rajh T. Fe_2O_3 nanoparticle structures investigated by X-ray absorption near-edge structure, surface modifications, and model calculations. *J Phys Chem B*. 2002;106(34):8539–8546.

38. Pirillo S, Cornaglia L, Ferreira ML, Rueda EH. Removal of fluorescein using different oxides as adsorbents: effect of pH. *Spectrochim Acta A*. 2008;71(2):636–643.

39. Roca AG, Marco JF, Morales MP, Serna CJ. Effect of nature and particle size on properties of uniform magnetite and maghemite nanoparticles. *J Phys Chem*. 2007;111(5):18577–18584.

40. Daou TJ, Greneche JM, Pourroy G, et al. Coupling agent effect on magnetic properties of functionalized magnetite-based nanoparticles. *Chem Mater*. 2008;20(18):5869–5875.

41. Kelkar SS, Reineke TM. Theranostics: combining imaging and therapy. *Bioconjug Chem*. 2011;22(10):1879–1903.

42. Duncan R, Gaspar R. Nanomedicine(s) under the microscope. *Mol Pharm*. 2011;8(6):2101–2141.

43. Bardocz S, Duguid TJ, Brown DS, et al. The importance of dietary polyamines in cell regeneration and growth. *Br J Nutr*. 1995;73(6):819–828.

44. Cipolla B, Guillè F, Moulinoux JP. Polyamine-reduced diet in metastatic hormone-refractory prostate cancer patients. *Biochem Soc Trans*. 2003;31(2):384–387.

45. Cipolla BG, Havouis R, Moulinoux JP. Polyamine contents in current foods: a basis for polyamine reduced diet and a study of its long term observance and tolerance in prostate carcinoma patients. *Amino Acids*. 2007;33(2):203–212.